

Exact sequence analysis for three-dimensional hydrophobic-polar lattice proteins

Reinhard Schiemann,^{a)} Michael Bachmann,^{b)} and Wolfhard Janke^{c)}

Institut für Theoretische Physik, Universität Leipzig, Augustusplatz 10/11, D-04109 Leipzig, Germany

(Received 4 May 2004; accepted 21 September 2004; published online 17 March 2005)

We have exactly enumerated all sequences and conformations of hydrophobic-polar (HP) proteins with chains of up to 19 monomers on the simple cubic lattice. For two variants of the HP model, where only two types of monomers are distinguished, we determined and statistically analyzed designing sequences, i.e., sequences that have a nondegenerate ground state. Furthermore we were interested in characteristic thermodynamic properties of HP proteins with designing sequences. In order to be able to perform these exact studies, we applied an efficient enumeration method based on contact sets. © 2005 American Institute of Physics. [DOI: 10.1063/1.1814941]

I. INTRODUCTION

Real proteins are built up of sequences of amino acids covalently linked by peptide bonds. Twenty different types of amino acids occurring in protein sequences are known. For a protein consisting of N amino acid residues there are thus, in principle, 20^N possibilities to form sequences or primary protein structures. Single domain polypeptides usually possess $N=30, \dots, 400$ residues; proteins built up of several domains can consist of up to 4000 amino acids. Only a few of the 20^N possible proteins, however, are actually realized in nature and are functional in a sense that they fulfil a specific task in a biological system. This requires the native structure of the protein to be unique and stable against moderate fluctuations of the environmental chemical and physical conditions. It is widely believed that the native state resides in a deep funnel-like minimum of the free energy landscape.¹ Since the energy of a protein depends on its sequence, it seems plausible that only such sequences of residues are favored whose associated energy landscape shows up a pronounced global minimum. On the other hand, from the conformational point of view, it can be estimated that the number of structures proteins typically fold into is only of the order of 1000—this is at least two orders of magnitude less than the number of known proteins.

Hence, exposing the nature of the relationship between sequences (primary structure) and conformations (secondary and higher structures) is one of the main aspects in protein research.² Attacking this general problem by means of computer simulations based on realistic interactions is currently impossible. There are two major obstacles being responsible for this. First, the precise form of the energy function in an all-atom approach containing all molecular and nuclear interactions within the polypeptide as well as the influence of the solvent is still under consideration. An important question is what “level of detail” is necessary to model proteins in gen-

eral. Considering an exemplified sequence of amino acid residues, the use of different force fields usually leads to different predictions of the native state. Second, even if a reliable model would exist, the sequence space is too large to be completely scanned by enumeration in order to search for the small number of sequences with appropriate free energy landscape (the number of primary structures of very short peptides with, say only ten residues, is $20^{10} \approx 10^{13}$).

In order to have a chance to perform such an analysis, the model must be drastically simplified. The simplest model to describe very qualitatively the folding behavior of proteins is the hydrophobic-polar (HP) model,³ where the continuous conformational space is reduced to discrete regular lattices and conformations of proteins are modeled as self-avoiding walks restricted to the lattice. In this model it is assumed that the hydrophobic interaction is the essential driving force towards the native fold. It is expected that the hydrophobic side chains are screened from the aqueous environment by hydrophilic residues. Therefore, the sequences of HP proteins consist of only two types of monomers (or classes of amino acids), amino acids with high hydrophobicity are treated as hydrophobic monomers (H), while the class of polar (or hydrophilic) residues is represented by polar monomers (P). In order to achieve the formation of a hydrophobic core surrounded by a shell of polar monomers, the interaction between hydrophobic monomers is attractive in the standard formulation of the model. All other interactions are neglected. Variants of the HP model also take into account (weaker) interactions between H and P monomers as well as between polar monomers.²

Although it is obvious that the HP model can describe the folding process very roughly only,^{4–7} much work has been done to find lowest-energy states and their degeneracy for given sequences, or in the inverse problem, to identify all sequences of given length whose native conformation matches a given target structure. As simple as this model seems to be, it has been proven to be an NP-complete problem in two and three dimensions.⁸ Therefore, sophisticated numerical algorithms were applied to find lowest-energy states for chains of up to 136 monomers. The algorithms

^{a)}Electronic mail: Reinhard.Schiemann@itp.uni-leipzig.de

^{b)}Electronic mail: Michael.Bachmann@itp.uni-leipzig.de

^{c)}Electronic mail: Wolfhard.Janke@itp.uni-leipzig.de. Homepage: <http://www.physik.uni-leipzig.de/CQT>

applied are based on very different methods, ranging from exact enumeration in two dimensions^{9,10} and three dimensions on cuboid (compact) lattices,^{2,11} and hydrophobic core construction methods^{12,13} over genetic algorithms,^{14–18} Monte Carlo simulations with different types of move sets,^{19–22} and generalized ensemble approaches²³ to Rosenbluth chain growth methods²⁴ of the *Go with the Winners* type.^{25–30} With some of these algorithms, thermodynamic quantities of lattice heteropolymers were studied as well.^{23,27,29–31}

In this work, we apply an exact enumeration method to three-dimensional HP proteins being not necessarily compact on the simple cubic (sc) lattice. For efficiency, we enumerated contact sets for chains of given length instead of conformations. In order to study the interplay between sequences and conformations and to investigate peculiarities of designing sequences, we performed a statistical analysis of the complete spaces of conformations and sequences for chains of up to $N=19$ monomers.

In Sec. II we give a review on the two variants of the HP model we use in our study, the original HP model and a variant taking into account an additional interaction between hydrophobic and polar residues. This is followed by Sec. III, where we discuss self-avoiding conformations and contact sets. Then, in Sec. IV, we perform an exact statistical analysis of properties of designing sequences and native conformations with lengths up to 19 monomers in comparison with the bulk of all possibilities to form sequences and to generate conformations, respectively. Since the exact data obtained with our algorithm can be rearranged in terms of the energy levels of the conformations, we are also able to determine the densities of states for all sequences. This allows for a study of the energetic thermodynamic properties of sequences whose associated ground state is unique or not, and their comparison from a thermodynamic point of view. We do just that in Sec. V. The paper is then concluded by summarizing our results in Sec. VI.

II. HP MODELS

A monomer of a HP sequence $\sigma=(\sigma_1, \sigma_2, \dots, \sigma_N)$ is characterized by its residual type ($\sigma_i=P$ for polar and $\sigma_i=H$ for hydrophobic residues), the place $1 \leq i \leq N$ within the chain of length N , and the spatial position \mathbf{x} to be measured in units of the lattice spacing. A conformation is then symbolized by the vector of the coordinates of successive monomers, $\mathbf{X}=(\mathbf{x}_1, \mathbf{x}_2, \dots, \mathbf{x}_N)$. We denote by $x_{ij}=|\mathbf{x}_i-\mathbf{x}_j|$ the distance between the i th and the j th monomer. The bond length between adjacent monomers in the chain is identical with the spacing of the used regular lattice with coordination number q . These covalent bonds are thus not stretchable. A monomer and its nonbonded nearest neighbors may form *contacts*. Therefore, the maximum number of contacts of a monomer within the chain is $(q-2)$ and $(q-1)$ for the monomers at the ends of the chain. To account for the excluded volume, lattice proteins are self-avoiding, i.e., two monomers cannot occupy the same lattice site. The general energy function of the noncovalent interactions reads in energy units ε (we set $\varepsilon=1$ in the following) as

$$E=\varepsilon \sum_{\langle i,j \rangle} C_{ij} U_{\sigma_i \sigma_j}, \quad (1)$$

where $C_{ij}=(1-\delta_{i+1j})\Delta(x_{ij}-1)$ with

$$\Delta(z)=\begin{cases} 1, & z=0 \\ 0, & z \neq 0 \end{cases} \quad (2)$$

is a symmetric $N \times N$ matrix called *contact map* and

$$U_{\sigma_i \sigma_j}=\begin{pmatrix} u_{HH} & u_{HP} \\ u_{HP} & u_{PP} \end{pmatrix} \quad (3)$$

is the 2×2 interaction matrix. Its elements $u_{\sigma_i \sigma_j}$ correspond to the energy of *HH*, *HP*, and *PP* contacts. For labeling purposes we shall adopt the convention that $\sigma_i=0 \triangleq P$ and $\sigma_i=1 \triangleq H$.

In the simplest formulation,³ which we will refer to as HP model in the following, only the attractive hydrophobic interaction is nonzero, $u_{HH}^{\text{HP}}=-1$, while $u_{HP}^{\text{HP}}=u_{PP}^{\text{HP}}=0$. Therefore, $U_{\sigma_i \sigma_j}^{\text{HP}}=-\delta_{\sigma_i H} \delta_{\sigma_j H}=-\sigma_i \sigma_j$. This model has been extensively used to identify ground states of HP sequences, some of which are believed to show up qualitative properties comparable with realistic proteins whose 20-letter sequence was translated into the two-letter code of the HP model.^{5,12,14,32,33} As we will see later on, this simple form of the HP model suffers, however, from the fact that the lowest-energy states are usually highly degenerate and therefore the number of designing sequences (i.e., sequences with unique ground state—up to the usual translational, rotational, and reflection symmetries) is very small, at least on the simple cubic lattice.

For a more reliable statistical sequence analysis, we compare with another model of HP type, as proposed in Ref. 2. This model was motivated by results from an analysis of inter-residue contact energies between real amino acids.³⁴ To this end, an attractive nonzero energy contribution for contacts between *H* and *P* monomers is assumed.² In what follows we call this the MHP (*mixed* HP) model. The elements of the interaction matrix (3) are chosen to be $u_{HH}^{\text{MHP}}=-1$, $u_{HP}^{\text{MHP}}=-1/2.3 \approx -0.435$, and $u_{PP}^{\text{MHP}}=0$.³⁵ The additional *HP* interaction breaks conformational symmetries yielding a much higher number of designing sequences on cubic lattices.

III. SELF-AVOIDING WALKS AND CONTACT MATRICES

Since lattice polymers are self-avoiding walks, the total number of conformations for a chain with N monomers is not known exactly. For $N \rightarrow \infty$ it is widely believed that in leading order the scaling law^{36,37}

$$C_n=A\mu_C^n n^{\gamma-1} \quad (4)$$

holds, where n is the number of self-avoiding steps (i.e., $n=N-1$). In this expression, μ_C is the effective coordination number of the lattice, γ is a universal exponent, and A is a nonuniversal amplitude. In Table I we have listed the exactly enumerated number for self-avoiding conformations of chains with up to $N=n+1=19$ monomers. Based on these data we estimated $\mu_C \approx 4.684$ and $\gamma \approx 1.16$ by extrapolating

TABLE I. Number of conformations C_N and contact matrices M_N for chains with N monomers (or, equivalently, self-avoiding walks with $n=N-1$ steps).

N	n	$\frac{1}{6}C_N$	M_N	$\frac{1}{6}C_N/M_N$
4	3	25	2	13
5	4	121	3	40
6	5	589	9	65
7	6	2821	20	141
8	7	13 565	66	206
9	8	64 661	188	344
10	9	308 981	699	442
11	10	1 468 313	2180	674
12	11	6 989 025	8738	800
13	12	33 140 457	29 779	1 113
14	13	157 329 085	121 872	1 290
15	14	744 818 613	434 313	1 715
16	15	3 529 191 009	1 806 495	1 954
17	16	16 686 979 329	6 601 370	2 528
18	17	78 955 042 017	27 519 000	2 869
19	18	372 953 947 349	102 111 542	3 652

the results obtained with the ratio method.^{36,38} These results are in good agreement with previous enumeration results,^{39–41} Monte Carlo methods⁴² and field-theoretic estimates⁴³ for γ . We should note that it is not the aim of this work to extend the numbers of walks C_N in Table I which has already been enumerated up to $n=26$ steps (and hence $C_{27} \approx 5.49 \times 10^{17}$ self-avoiding conformations with $N=27$ monomers).⁴⁰ Rather, we scan the combined space of HP sequences and conformations which contains for chains of $N=19$ monomers $2^{19}C_{19} \approx 1.17 \times 10^{18}$ possible combinations. Therefore, the computational effort of our study is comparably demanding.

In models with the general form (1), where the calculation of the energy reduces to the summation over contacts (i.e., pairs of monomers being nearest neighbors on the lattice but nonadjacent along the chain) of a given conformation, the number of conformations that must necessarily be enumerated can drastically be decreased by considering only classes of conformations, so-called contact sets.^{10,44} A contact set is uniquely characterized by a corresponding contact map (or contact matrix), but a single conformation is not. Thus, for determining energetic quantities of different sequences, it is sufficient to carry out enumerations over contact sets. In a first step, however, the contact sets and their degeneracy, i.e., the number of conformations belonging to each set, must be determined and stored. Then, the loop over all nonredundant sequences is performed for all contact sets instead of conformations. The technical details of our implementation will be described elsewhere.⁴⁵

In Table I, the resulting numbers of contact sets M_N are summarized and, although also growing exponentially [see Figs. 1(a) and 1(b)], the gain of efficiency by enumerating contact sets is documented by the ratio between C_N and M_N in the last column. Assuming that the number of contact sets M_n follows a scaling law similar to Eq. (4), we estimated the effective coordination number to be approximately $\mu_M \approx 4.38$. Unfortunately, the ratios of numbers of contact sets for even and odd numbers of walks oscillate much stronger

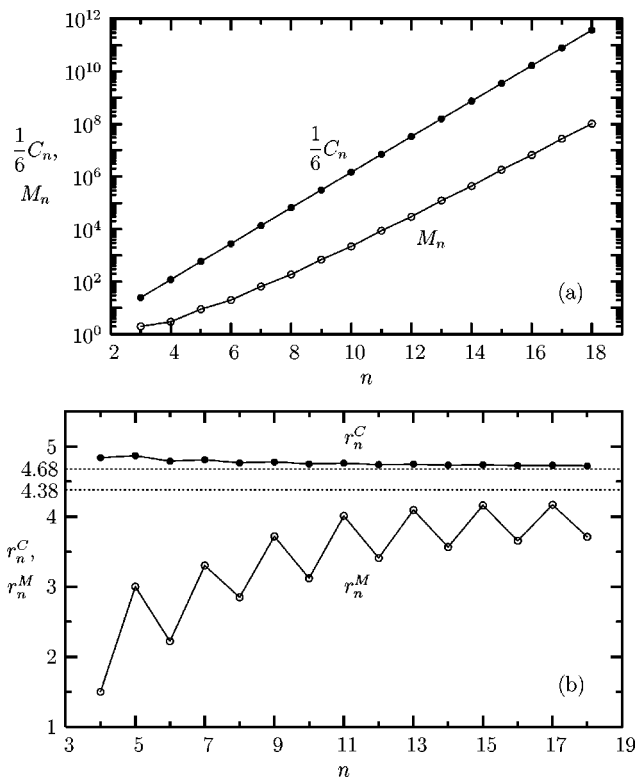


FIG. 1. (a) Dependence of the numbers of self-avoiding walks C_n and contact matrices M_n on the number of steps $n=N-1$. (b) Ratios of numbers of self-avoiding walks $r_n^C=C_n/C_{n-1}$ and contact matrices $r_n^M=M_n/M_{n-1}$. The dotted lines indicate the values the respective series converge to, $r_\infty^C=\mu_C \approx 4.68$ and $r_\infty^M=\mu_M \approx 4.38$, respectively.

than for the number of conformations, as shown in Fig. 1(b). This renders an accurate scaling analysis (in particular, for the exponent γ) based on the data for the relatively small number of steps much more difficult than for self-avoiding walks.

IV. EXACT STATISTICAL ANALYSIS OF DESIGNING SEQUENCES

In this section, we analyze the complete sets S_N of designing sequences for HP proteins of given numbers of residues $N \leq 19$. A sequence σ is called *designing*, if there is only one conformation associated with the native ground state, not counting rotation, translation, and reflection symmetries that altogether contribute on a simple cubic lattice a symmetry factor 6 for linear, 24 for planar, and 48 for conformations spreading into all three spatial directions. In Table II we have listed the numbers of designing sequences S_N we found for the two models. In contrast to previous investigations of HP proteins on the square lattice,¹⁰ the number of designing sequences obtained with the pure HP model is extremely small on the simple cubic lattice. This does not allow for a reasonable statistical study of general properties of designing sequences, at least for very short chains. The situation is much better using the more adequate MHP model. The first quantity under consideration is the hydrophobicity of a sequence σ , i.e., the number of hydrophobic monomers N_H , normalized with respect to the total number of residues,

TABLE II. Number of designing sequences S_N (only relevant sequences, see text) in the HP and MHP models.

N	4	5	6	7	8	9	10	11	12	13	14	15	16	17	18	19
S_N^{HP}	3	0	0	0	2	0	0	0	2	0	1	1	1	8	29	47
S_N^{MHP}	7	0	0	6	13	0	11	8	124	14	66	97	486	2196	9491	4885

$$m(\boldsymbol{\sigma}) = \frac{N_H}{N} = \frac{1}{N} \sum_{i=1}^N \sigma_i. \quad (5)$$

The average hydrophobicity over a set of designing sequences of given length N is then defined by

$$\langle m \rangle_N = \frac{1}{S_N} \sum_{\boldsymbol{\sigma} \in S_N} m(\boldsymbol{\sigma}). \quad (6)$$

In Fig. 2 we have plotted $\langle m \rangle_N$ as function of the sequence length N . The plots do not show up a clear tendency to what average hydrophobicity they converge for long chains. This to know would be, however, of some interest for the design of a biased algorithm of Monte Carlo type that searches the combined sequence and conformational space for candidates of designing sequences with lengths, where enumeration is no longer applicable. A distinct indication that designing sequences have in most cases hydrophobicities different from 0.5 could be used as a bias in order to reduce the section of the sequence space to be scanned, since the number of all possible sequences with given hydrophobicity has a peak at $m=0.5$ [see Fig. 3(a)] which becomes the more pronounced the higher the number of residues is.

It should be noted that the hydrophobicity distribution for all these sequences is not binomial since in our analysis we have distinguished only sequences that we call *relevant*, i.e., two sequences that are symmetric under reversal of their residues are identified and enter only once into the statistics. Therefore we consider, for example, only ten relevant sequences with length $N=4$ instead of $2^4=16$. Taking into account *all* 2^N sequences would obviously lead to a binomial distribution for N_H , since there are then exactly

$$\binom{N}{N_H} \quad (7)$$

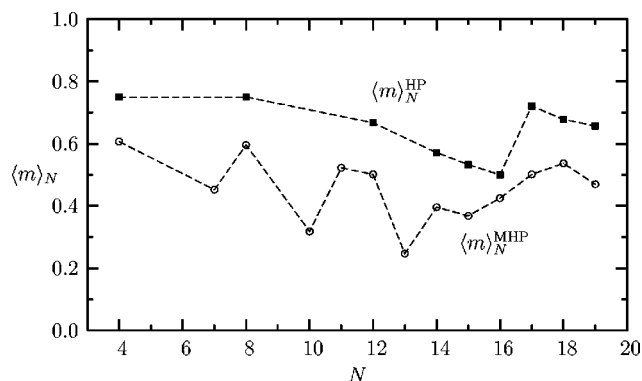


FIG. 2. Dependence of average hydrophobicities $\langle m \rangle_N$ for designing sequences on the sequence length N in both models. For several chain lengths, where no designing sequences exist (see Table II), the calculation of the average hydrophobicity (6) does not make sense. The dashed lines are therefore only guides to the eye.

sequences with N_H hydrophobic monomers.

In Fig. 3(a) we have plotted both the distribution of hydrophobicity of the designing sequences with $N=18$ monomers in the MHP model and, for comparison, the distribution of all sequences with $N=18$. For this example, we see that the width (or standard deviation) of the hydrophobicity distribution for the designing sequences, which has its peak at $\langle m \rangle_{18}^{\text{MHP}} \approx 0.537 > 0.5$, is smaller than that of the distribution over all sequences. In order to gain more insight how the hydrophobicity distributions differ, we have compared the widths of both distributions in their dependence on the chain length $N \leq 19$. This is shown in Fig. 3(b). It seems that for $N \rightarrow \infty$ the widths of the hydrophobicity distributions for the designing sequences asymptotically approach the curve of the widths of the hydrophobicity distributions of all sequences.

The hydrophobicity profile

$$p_i = \frac{1}{2S_N} \sum_{\boldsymbol{\sigma} \in S_N} (\sigma_i + \sigma_{N-i+1}), \quad i=1,2,\dots,N, \quad (8)$$

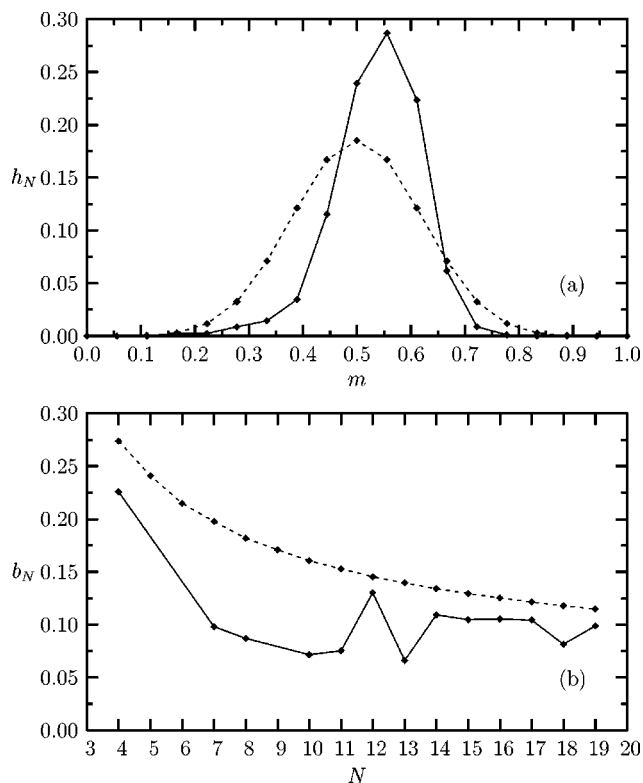


FIG. 3. (a) Distribution of hydrophobicity h_N of all designing sequences with $N=18$ monomers (solid line) compared with the distribution of hydrophobicity of all sequences of this length (dashed line) for the MHP model. (b) Widths of the hydrophobicity distribution of the designing sequences, b_N , depending on the chain length N (solid line) compared with the widths of the hydrophobicity distribution of all sequences (dashed line) for the MHP model.

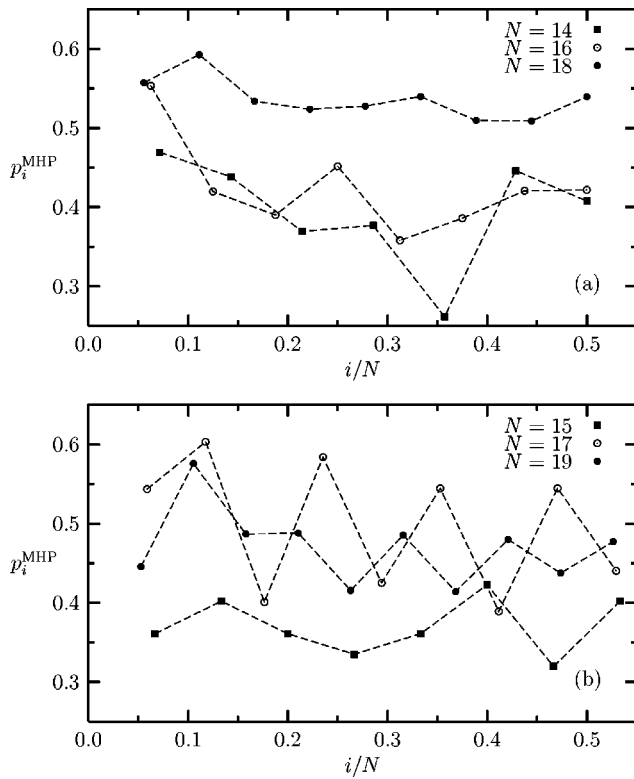


FIG. 4. Hydrophobicity profiles p_i for designing sequences with (a) even and (b) odd numbers of monomers in the MHP model. Since the profile (8) is symmetric under $i \leftrightarrow N-i+1$ we have only plotted it for half the chain.

is a measure for the probability to find a hydrophobic monomer in a distance i from the nearest end of a designing sequence. Thus, this quantity gives an impression of how the H monomers are on average distributed along the chain. In Figs. 4(a) and 4(b) the profiles for designing sequences in the MHP model are plotted for respective chains with even ($N = 14, 16, 18$) and odd numbers ($N = 15, 17, 19$) of residues. As a first remarkable result, we see that for odd numbers of monomers [Fig. 4(b)] the profile shows up periodic oscillations, i.e., if the n th monomer is preferably hydrophobic the $(n+1)$ th residue is with lower probability. As this effect is stronger for $N=17$ than for $N=19$, we expect that the amplitude of these oscillations decreases with increasing number of monomers. The behavior of the chains with even number of monomers [Fig. 4(a)] is less spectacular. Here, for increasing number of monomers, the probability seems to become more and more equally distributed. Therefore, it is more interesting to study how each monomer of the designing sequences is involved in the formation of HH contacts (as well as HP contacts in the MHP model) being favored in low-energy conformations. To this end, we define the hydrophobic contact density profile by

$$q_i = \frac{1}{2S_N} \sum_{\sigma \in S_N} \sum_{j=1}^N [C_{ij} \sigma_i \sigma_j + C_{N-i+1j} \sigma_{N-i+1} \sigma_j], \quad (9)$$

where C_{ij} is the contact map defined after Eq. (1). The higher the affinity of the i th monomer to form contacts (preferably if it is hydrophobic) the bigger the value of q_i . This profile is shown in Fig. 5 for both models, where we have

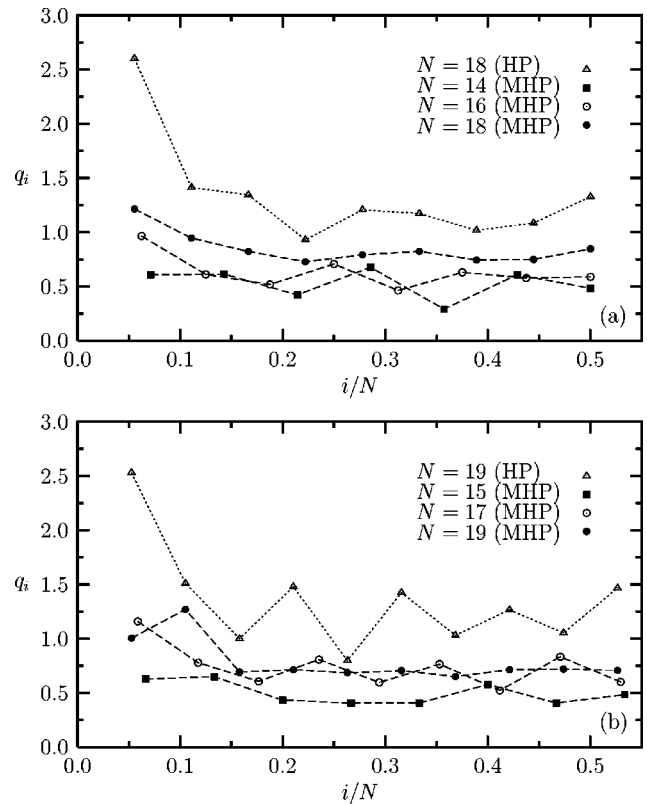


FIG. 5. Profiles of the contact density q_i for designing sequences with (a) even and (b) odd numbers of monomers in the MHP model. For comparison, we have also inserted the profiles obtained in the HP model for $N=18$ and $N=19$, respectively. By definition (9), this profile is also symmetric under $i \leftrightarrow N-i+1$.

again separated even and odd numbers of residues. From the two profiles for the HP model ($N=18, 19$), we observe that there is a strong tendency of the monomers at the ends of the chain ($i=1, N$) to form hydrophobic (HH) contacts. The reason is that these two monomers can have five nearest neighbors on the sc lattice, i.e., there is one more possibility for them to form a favorable energetic contact than for monomers residing within the chain. In the MHP model, this behavior is less pronounced, since also HP contacts are attractive and the tendency that the ends are preferably hydrophobic is much weaker.

After having discussed sequential properties of designing sequences, we now analyze the properties of their unique ground-state structures, the native conformations. From Table III we read off that the number of *different* native conformations D_N is usually much smaller than the number of designing sequences, i.e., several designing sequences share the same ground-state conformation. The number of designing sequences that fold into a certain given target conformation $\mathbf{X}^{(0)}$ (or conformations being trivially symmetric to this by translations, rotations, and reflections) is called *designability*,⁴⁶

$$F_N(\mathbf{X}^{(0)}) = \sum_{\sigma \in S_N} \Delta(\mathbf{X}_{\text{gs}}(\sigma) - \mathbf{X}^{(0)}), \quad (10)$$

where $\mathbf{X}_{\text{gs}}(\sigma)$ is the native (ground-state) conformation of

TABLE III. Number of designable conformations D_N in both models.

N	4	5	6	7	8	9	10	11	12	13	14	15	16	17	18	19
D_N^{HP}	1	0	0	0	2	0	0	0	2	0	1	1	1	8	28	42
D_N^{MHP}	1	0	0	2	2	0	5	6	30	8	31	58	258	708	1447	1623

the designing sequence σ . The function $\Delta(\mathbf{Z})$ is the generalization of Eq. (2) to $3N$ -dimensional vectors. It is unity for $\mathbf{Z}=\mathbf{0}$ and zero otherwise.

The designability is plotted in Fig. 6 for all native conformations that HP proteins with $N=17$, 18, and 19 monomers can form in the MHP model. In this figure, the abscissa is the rank of the conformations, ordered according to their designability. The conformation with the lowest rank is therefore the most designable structure and we see that a majority of the designing sequences folds into a few highly designable conformations, while only a small number of designing sequences possesses a native conformation with low designability (note that the plot is logarithmic). Similar results were found, for example, in Ref. 47, where the designability of compact conformations on cuboid lattices was investigated in detail. The left picture in Fig. 7 shows the conformation with the lowest rank (or highest designability) with $N=18$ monomers.

From our analysis we see that this characteristic distribution of the designing sequences is not restricted to cuboid lattices only. This result is less trivial than one may think at first sight. As we will show later on in this paper in the discussion of the radius of gyration, native conformations are very compact, but only very few conformations are maximally compact (at least for $N \leq 19$). For longer sequences similar results were found in Ref. 30. Highly designable conformations are of great interest, since it is expected that they form a frame making them stable against mutations and thermodynamic fluctuations. Such fundamental structures are also relevant in nature, where, in particular, secondary structures (helices, sheets, hairpins) supply proteins with a stable backbone.⁴⁷

Conformational properties of polymers are usually studied in terms of the squared end-to-end distance

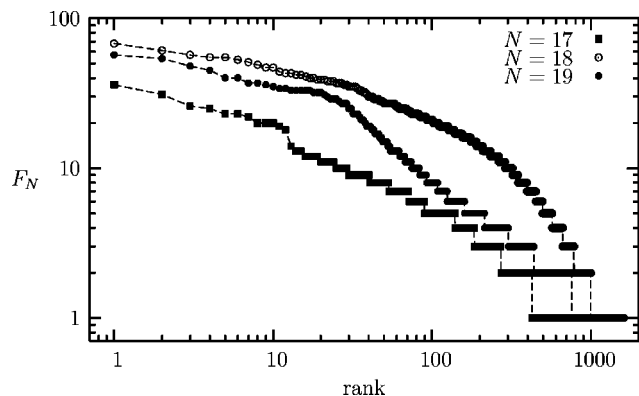


FIG. 6. Designability F_N of native conformations in the MHP model for $N=17$, 18, and 19. The abscissa is the rank obtained by ordering all designable conformations according to their designability.

$$R_e^2 = (\mathbf{x}_N - \mathbf{x}_1)^2 \quad (11)$$

and the squared radius of gyration

$$R_g^2 = \frac{1}{N} \sum_{i=1}^N (\mathbf{x}_i - \bar{\mathbf{x}})^2, \quad (12)$$

where $\bar{\mathbf{x}} = \sum_i \mathbf{x}_i / N$ is the center of mass of the polymer. In polymer physics both quantities are usually referred to as measures for the compactness of a conformation. A typical conformation with minimal radius of gyration for a chain with $N=18$ monomers is shown in the right picture of Fig. 7.

In Fig. 8(a) we compare the N -dependence of the averages of the native conformations found in the MHP model and all possible self-avoiding walks (SAW). The same quantities for the squared radius of gyration are shown in Fig. 8(b). The averages were obtained by calculating

$$\langle R_{e,g}^2 \rangle^{\text{SAW}} = \frac{1}{C_N} \sum_{\mathbf{X} \in C_N} R_{e,g}^2(\mathbf{X}), \quad (13)$$

$$\langle R_{e,g}^2 \rangle^{\text{MHP}} = \frac{1}{S_N} \sum_{\sigma \in S_N} R_{e,g}^2(\mathbf{X}_{\text{gs}}(\sigma)), \quad (14)$$

where C_N is the set of all self-avoiding conformations on a sc lattice. Figure 8(a) shows for the mixed HP model that, compared to $\langle R_{e,g}^2 \rangle^{\text{SAW}} \sim n^{2\nu}$ with $\nu \approx 0.59$ (see Ref. 48 for a recent summary of estimates for ν), the average end-to-end distance $\langle R_{e,g}^2 \rangle^{\text{MHP}}$ of the native conformations only is much smaller. For even number of monomers, the ends of a HP protein can form contacts with each other on the sc lattice. Accordingly, the values of $\langle R_{e,g}^2 \rangle^{\text{MHP}}$ are smaller for N being even and the even-odd oscillations are very pronounced. The widths $b_{R_e^2}$ of the distributions of the squared end-to-end distances are also very small. Even for heteropolymers with $N=19$ monomers in total, there are virtually no native conformations, where the distance between the ends is larger than three lattice sites. We have checked this for the standard HP model, too, and found the same effect. Since the number of native conformations is very small in this model, we have

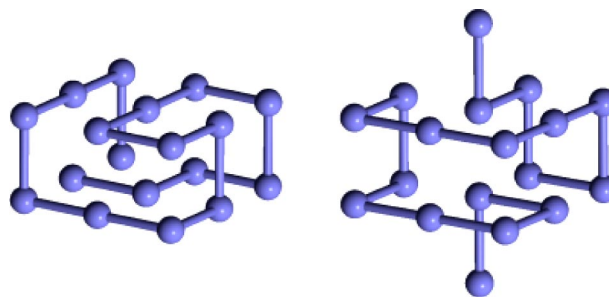


FIG. 7. Structure ($N=18$) with the highest designability of all native conformations (left) and with minimal radius of gyration (right).

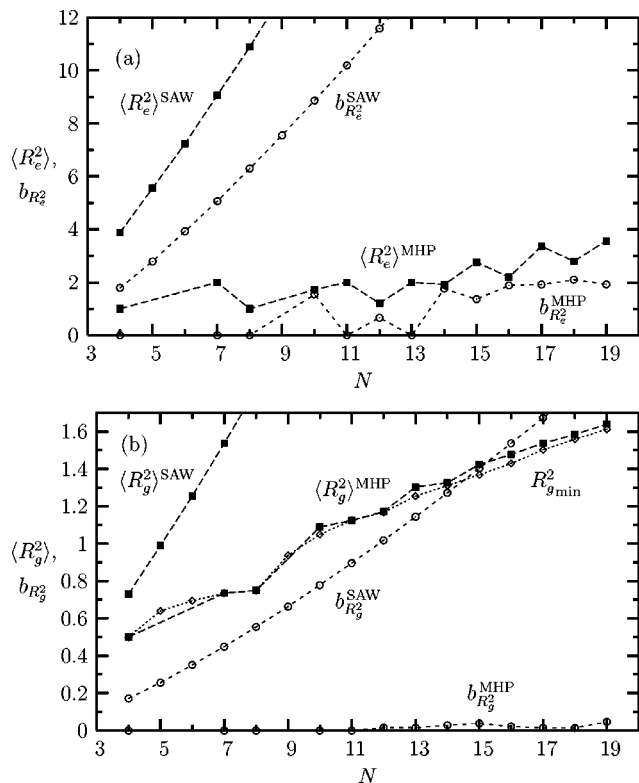


FIG. 8. (a) Average squared end-to-end distances $\langle R_e^2 \rangle$ of native conformations in the MHP model compared with those of all self-avoiding walks (SAW). We have also inserted the widths $b_{R_e^2}$ of the corresponding distributions of end-to-end distances. (b) The same for the average squared radius of gyration $\langle R_g^2 \rangle$. Since the radius of gyration is an appropriate measure for the compactness of a conformation, we have also plotted $R_{g,\min}^2$ for the conformations with the minimal radius of gyration (or, equivalently, maximal compactness).

not included these results in the figure. Depicting the average squared radius of gyration $\langle R_g^2 \rangle$ and the widths of the corresponding distribution of the radius of gyration in Fig. 8(b) for all self-avoiding conformations as well as for the native ones, we see that these results confirm the above remarks. As the average end-to-end distances of native conformations are much smaller than those for the bulk of all conformations, we observe the same trend for the mean squared radii of gyration $\langle R_g^2 \rangle^{\text{MHP}}$ and $\langle R_g^2 \rangle^{\text{SAW}}$ and the widths $b_{R_g^2}^{\text{MHP}}$ and $b_{R_g^2}^{\text{SAW}}$ as well. In particular, the width $b_{R_g^2}^{\text{MHP}}$ is so small, that virtually all native conformations possess the same radius of gyration. For this reason, we have also searched for the conformations having the smallest radius of gyration $R_{g,\min}^2$ (these conformations are not necessarily native as we will see!) and inserted these values into this figure, too. We observe that these values differ only slightly from $\langle R_g^2 \rangle^{\text{MHP}}$. Thus we conclude that native conformations are very compact but not necessarily maximally compact. This property has already been utilized in enumerations being performed *a priori* on compact lattices,^{2,11,47} where the proteins are confined by hand to live in small cuboids (e.g., of size $3 \times 3 \times 3$ or $4 \times 3 \times 3$). Our results on the general sc lattice confirm that this assumption is justified to a great extent. Nevertheless, the slight deviation from the minimal radius of

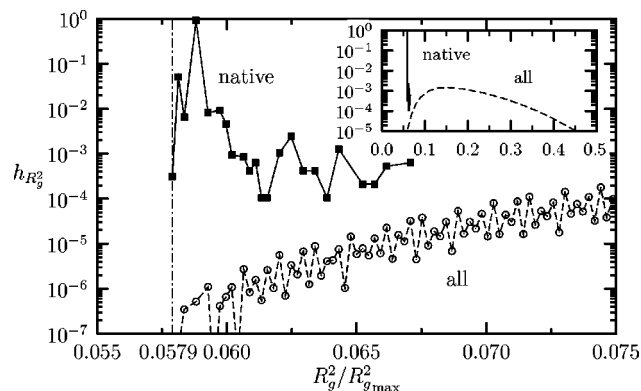


FIG. 9. Distribution $h_{R_g^2}$ (normalized to $\sum h_{R_g^2} = 1$) of squared radii of gyration (normalized with respect to the maximal radius of gyration $R_{g,\max}^2 = (N^2 - 1)/12$ of a completely stretched conformation) of native conformations with $N = 18$ in the MHP model, compared with the histogram for all self-avoiding conformations. The vertical line refers to the minimal radius of gyration ($R_{g,\min}^2/R_{g,\max}^2 = 0.0579$ for $N = 18$) and an associated structure is shown on the right-hand side of Fig. 7. The inset shows the distribution up to $R_g^2/R_{g,\max}^2 = 0.5$.

gyration native conformations exhibit is a remarkable result as it concerns about 90% of the whole set of native conformations! This can be seen in Fig. 9, where we have plotted the distribution of the squared radii of gyration for all self-avoiding conformations with $N = 18$ and the native states in the MHP model. All native conformations have a very small radius of gyration but only a few of them share the smallest possible value. A structure with the smallest radius of gyration is shown on the right-hand side of Fig. 7. It obviously differs from the most-designable conformation drawn on the left of the same figure.

V. DENSITY OF STATES AND THERMODYNAMICS

In this section we systematically compare energetic thermodynamic quantities of designing and nondesigning sequences. In Ref. 49 it was conjectured for exemplified sequences of comparable 14mers, one of them being designing, that designing sequences in the HP model seem to show up a much more pronounced low-temperature peak in the specific heat than the nondesigning examples. This peak may be interpreted as kind of a conformational transition between structures with compact hydrophobic cores (ground states) and states where the whole conformation is highly compact (globules).^{29,30} Another peak in the specific heat at higher temperatures, which is exhibited by all lattice proteins, is an indication for the usual globule—coil transition between compact and untangled conformations.

In order to study energetic thermodynamic quantities, such as mean energy and specific heat, we determined from our enumerated conformations for a given sequence the density of states $g(E)$ that conveniently allows the calculation of the partition sum $Z(T) = \sum_E g(E) \exp(-E/k_B T)$ and the moments $\langle E^k \rangle_T = \sum_E E^k g(E) \exp(-E/k_B T) / Z$, where the subscript T indicates the difference of calculating thermal mean values based on the Boltzmann probability from averages previously introduced in this paper. Then the specific heat is given by the fluctuation formula $C_V = (\langle E^2 \rangle_T - \langle E \rangle_T^2) / k_B T^2$.

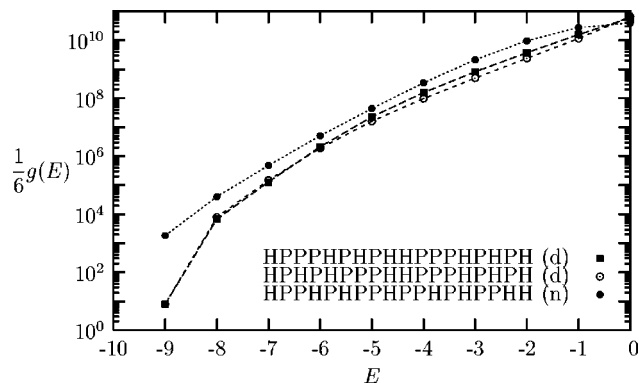


FIG. 10. Density of states $g(E)$ for two designing sequences (d) with $N = 18$, $m_H = 8$, and $E_{\min} = -9$ in the HP model. We have divided out the symmetry factor 6 that is common to all conformations. Three-dimensional conformations have an additional symmetry factor 8, such that the states with minimal energy for these two curves are indeed unique and the sequences are designing. For comparison we have also plotted $g(E)$ for one exemplified non-designing sequence (n) out of 525 having the same properties as quoted above, but different sequences. The ground-state degeneracy for this example is $g_0 = g(E_{\min}) = 6 \times 1840$ (including all symmetries).

A. Sequences in the HP model

In the HP model with pure hydrophobic interaction the density of states shows up a monotonic growth with increasing energy, at least for the short chains in our study (for longer chains, e.g., the 42mer investigated in Refs. 29 and 30, the number of states in the high-energy region decreases, i.e., the density of states possesses a global maximum at an energy E residing within the interval $E_{\min} < E < E_{\max} = 0$). For a reasonable comparison of the behavior of designing and non-designing sequences, we have focused on 18mers having the same hydrophobicity ($m_H = 8$) and ground-state energy $E_{\min} = -9$. There are in total 527 sequences with these properties, two of which are designing. The densities of states for the two designing sequences and an example of a non-designing sequence are plotted in Fig. 10. We have already divided out a global symmetry factor 6 (number of possible directions for the link connecting the first two monomers) that all conformations on a sc lattice have in common. Since the ground-state conformations of the designing sequences spread into all three dimensions, an additional symmetry factor $4 \times 2 = 8$ (four for rotations around the first bond, two for a remaining independent reflection) makes a number of conformations obsolete and the ground-state degeneracy of the designing sequences is indeed unity. Obviously this is not the case for the sequences we identified as non-designing. In fact, the uniqueness of the ground states of designing sequences is a remarkable property as there are not less than $\sim 10^{10}$ possible conformations of HP lattice proteins with 18 monomers. As we also see in Fig. 10, the ratio of the density of the first excited state ($E = -8$) for the designing and the non-designing sequences is smaller than for the ground state. This means that, at least for these short chains, the low-temperature behavior of the HP proteins in this model strongly depends on the degeneracy of the ground state. Furthermore, we expect that the low-temperature behavior of both designing sequences is very similar as their low-energy densities hardly differ. We have investigated this, once more

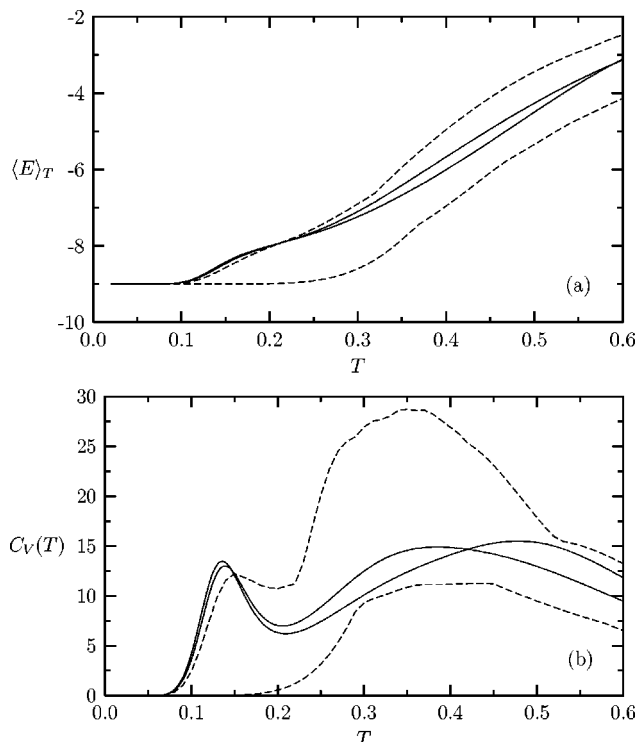


FIG. 11. (a) Mean energy $\langle E \rangle_T$ and (b) specific heat C_V for the two designing sequences with $N = 18$, $m_H = 8$, and $E_{\min} = -9$ (solid lines) in the HP model, whose densities of states were plotted in Fig. 10. The curves of the same quantities for the 525 non-designing sequences are completely included within the respective areas between the dashed lines. The low-temperature peak of the specific heat (near $T = 0.14$) is most pronounced for the two designing sequences which behave similarly for low temperatures.

for the 18mers with the properties described above, by considering the mean energy $\langle E \rangle_T$ and the specific heat $C_V(T)$. The results are shown in Figs. 11(a) and 11(b), respectively. The two solid curves belong to the two designing sequences and the dashed lines are the minimum/maximum bounds of the respective quantities for the non-designing sequences. As a main result we find that designing and non-designing sequences behave indeed differently for very low temperatures. There is a characteristic, pronounced low-temperature peak in the specific heat that can be interpreted as kind of transition between low-energy states with hydrophobic core and very compact globules. This confirms a similar observation for the 14mers studied in Ref. 49.

The upper bound of the specific heats for non-designing sequences in Fig. 11(b) exposes two peaks. By analyzing our data for all 525 non-designing sequences we found that there are two groups: some of them experience two conformational transitions while others do not show a characteristic low-temperature behavior. Thus, the only appearance of these two peaks is not a unique, characteristic property of designing sequences. In order to quantify this observation, we have studied all relevant 32896 sequences with 16 monomers. Only one of these sequences is designing ($HP_2HP_2HPPH_2PHPH$, with minimum energy $E_{\min} = -9$), but in total there are 593 sequences, i.e., 1.8% of the relevant sequences, corresponding to curves of specific heats with two local maxima. It should be noted that the

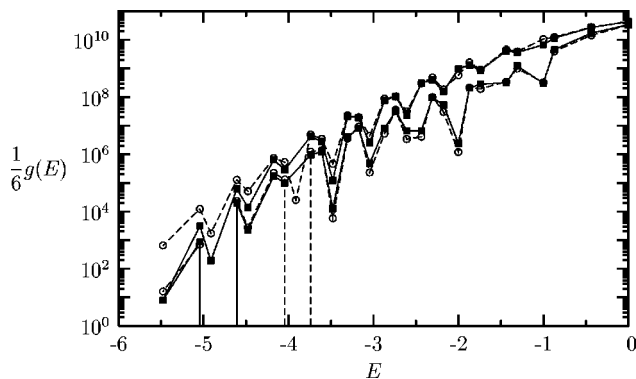


FIG. 12. Minimum and maximum boundaries for the densities of states of the 13 designing (filled boxes, connected by solid lines) and the 40 nondesigning sequences (open circles, connected by dashed lines) with 18 monomers, hydrophobicity $m_H=3$, and ground-state energy $E_{\min} \approx -5.478$ in the MHP model. Once more, a global symmetry factor 6 has already been divided out.

degeneracies of the ground states associated with these sequences are comparably small.

B. Properties of the MHP model

In the MHP model, the energy levels are no longer equally spaced due to the additional noninteger HP interaction. Moreover, the absolute value of the energy of the lattice heteropolymer is not necessarily identical with the number of hydrophobic contacts. The formation of a highly compact core is still energetically favored, but also the attractive contacts between H and P monomers reduce the energy of the heteropolymer. For this reason, the relatively manifest distinction between “phases” with compact H -core states and entirely compact conformations is expected to be much less pronounced, even for the designing sequences.

Once more, we have first enumerated the densities of states for a set of sequences that have similar properties but differ only in the ordering of the sequence. For this study we chose all 18mers sharing the same hydrophobicity $m_H=3$ and identical ground-state energy $E_{\min}=2u_{HH}^{\text{MHP}}+8u_{HP}^{\text{MHP}} \approx -5.478$, since there are two HH and eight HP contacts in each of the ground-state conformations. We found 13 designing and 40 nondesigning sequences that satisfy these specifications. In order not to be confused by too many curves, in Fig. 12 again only the minimum and maximum boundaries of the designing sequences (solid lines) are shown as well as the corresponding bounds for the nondesigning sequences (dashed lines). We observe that the regions enclosed by the boundaries do not exhibit significant differences in both cases except for the ground-state energy E_{\min} , where the ground-state degeneracy for the designing sequences is $g_0^{\text{d}} = g_{0,\min}^{\text{d}} = g_{0,\max}^{\text{d}} = 48$ (i.e., identical with the global symmetry factor for three-dimensional conformations), while the degeneracies for the nondesigning sequences lie within the interval $g_{0,\min}^{\text{n}} = 96 \leq g_0^{\text{n}} \leq g_{0,\max}^{\text{n}} = 3888$. Note that $g_{\min}^{\text{d}}(E \approx -3.913) = 0$ and $g_{\min}^{\text{n}}(E \approx -4.913) = g_{\min}^{\text{n}}(E \approx -4.913) = 0$. Interestingly, the state with energy $E \approx -3.913$ is never occupied by the designing sequences, in contrast to the nondesigning sequences.

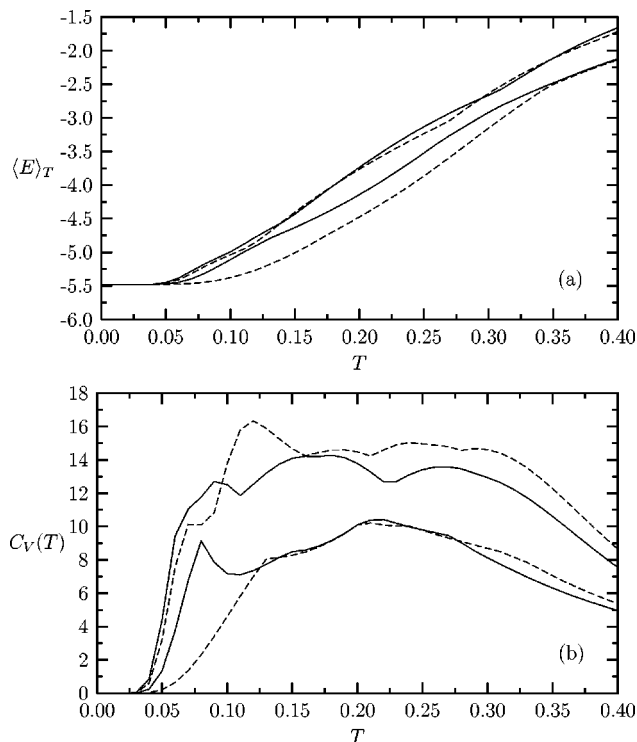


FIG. 13. Minimum and maximum boundaries of the (a) mean energy $\langle E \rangle_T$ and (b) specific heat C_V for the designing (solid lines) and nondesigning sequences (dashed lines) in the MHP model, with the properties listed in the caption of Fig. 12.

Since the densities of states for designing and nondesigning sequences hardly differ, it is difficult to identify a particular thermodynamic behavior being characteristic for designing sequences only. This is indeed true as can be seen from Figs. 13(a) and 13(b), where we have plotted the lower and upper boundaries for the respective mean energies and specific heats of these 18mers. In contrast to the results for the HP model [cf. Figs. 11(a) and 11(b)], where, within a certain low-temperature interval, the regions enclosing the curves for the designing and nondesigning sequences do not overlap, a separation of this kind is not apparent in the MHP model. Nevertheless, these figures also show that for very low temperatures ($0 < T < 0.1$), the general behavior is very similar for all designing sequences, but it is not for the nondesigning sequences, where the temperature dependence of energy and thus specific heat can be significantly different.

VI. SUMMARY

We have exactly analyzed the combined space of sequences and conformations for proteins on the simple cubic lattice for two HP-type models that differ in the contact energy between hydrophobic and polar monomers. In the original HP model³ this interaction is zero, while in the more realistic MHP model² there is a nonzero contribution as suggested by the Miyazawa-Jernigan matrix of contact energies between amino acids in proteins.³⁴ Since there were only a few known exact results for heteropolymers in three dimensions, mainly on compact cuboid lattices, we generated by exact enumeration the sets of designing sequences and native conformations on noncompact simple cubic lattices. We

studied, how their properties, measured, e.g., in terms of quantities like designability, end-to-end distance, radius of gyration, etc., differ from the bulk of all possible sequences and all self-avoiding conformations, respectively. We found that ground states of designing sequences, i.e., native conformations, have a much smaller mean end-to-end distance than the set of all conformations with the same length. Moreover, we confirmed that these conformations are very compact, i.e., they have a smaller mean radius of gyration than the whole set. This is valid for both models under consideration.

We have also studied energetic thermodynamic properties, in order to investigate how characteristic the low-temperature behavior of designing compared to nondesigning sequences is. We determined the densities of states for respective sets of selected 18mers with comparable properties. In the HP model, where the number of designing sequences is rather small compared with the MHP model, we could observe that energetic fluctuations are different for designing and nondesigning sequences within a certain low-temperature region. Designing sequences show up a more pronounced low-temperature peak in the specific heat being related to a conformational transition between low-energy states with hydrophobic core and highly compact globules. For the MHP model the situation is more diffuse, and a clear distinction between designing and nondesigning sequences based on characteristic thermodynamic properties is not possible. Nevertheless, we have also seen in this model that designing sequences behave similarly for very low temperature while nondesigning sequences react quite differently on changes of the temperature, over the entire range of temperatures.

ACKNOWLEDGMENTS

This work was partially supported by the German-Israel-Foundation (GIF) under Contract No. I-653-181.14/1999. One of us (R.S.) acknowledges support by the Studienstiftung des deutschen Volkes.

- ¹K. A. Dill, *Protein Sci.* **8**, 1166 (1999).
- ²C. Tang, *Physica A* **288**, 31 (2000).
- ³K. A. Dill, *Biochemistry* **24**, 1501 (1985); K. F. Lau and K. A. Dill, *Macromolecules* **22**, 3986 (1989).
- ⁴E. I. Shakhnovich, *Phys. Rev. Lett.* **72**, 3907 (1994).
- ⁵K. Yue, K. M. Fiebig, P. D. Thomas, H. S. Chan, E. I. Shakhnovich, and K. A. Dill, *Proc. Natl. Acad. Sci. U.S.A.* **92**, 325 (1995).
- ⁶M. Vendruscolo and E. Domany, *J. Chem. Phys.* **109**, 11101 (1998).
- ⁷H. S. Chan and E. Bornberg-Bauer, *Applied Bioinformatics* **1**, 121 (2002).
- ⁸B. Berger and T. Leighton, *J. Comput. Biol.* **5**, 27 (1998); P. Crescenzi, D. Goldman, C. Papadimitriou, A. Piccolboni, and M. Yannakakis, *ibid.* **5**, 423 (1998).
- ⁹A. Irbäck and E. Sandelin, *J. Chem. Phys.* **108**, 2245 (1998).
- ¹⁰A. Irbäck and C. Troein, *J. Biol. Phys.* **28**, 1 (2002).
- ¹¹H. Cejtin, J. Edler, A. Gottlieb, R. Helling, H. Li, J. Philbin, C. Tang, and N. Wingreen, *J. Chem. Phys.* **116**, 352 (2002).
- ¹²K. Yue and K. A. Dill, *Phys. Rev. E* **48**, 2267 (1993); *Proc. Natl. Acad. Sci. U.S.A.* **92**, 146 (1995).
- ¹³T. C. Beutler and K. A. Dill, *Protein Sci.* **5**, 2037 (1996).
- ¹⁴R. Unger and J. Moulton, *J. Mol. Biol.* **231**, 75 (1993).
- ¹⁵N. Krasnogor, W. E. Hart, J. Smith, and D. A. Pelta, in *Proceedings of the Genetic and Evolutionary Computation Conference (GECCO99)*, Orlando, FL, edited by W. Banzhaf, J. Daida, A. E. Eiben, M. H. Garzon, V. Honavar, M. Jakiela, and R. E. Smith (Morgan Kaufmann, San Francisco, 1999), p. 1596.
- ¹⁶Y. Cui, W. H. Wong, E. Bornberg-Bauer, and H. S. Chan, *Proc. Natl. Acad. Sci. U.S.A.* **99**, 809 (2002).
- ¹⁷N. Lesh, M. Mitzenmacher, and S. Whitesides, in *Proceedings of the Seventh Annual International Conference on Computational Molecular Biology (RECOMB03)*, Berlin, edited by M. Vingrom, S. Istrail, P. Pevzner, and M. Waterman (ACM, New York, 2003), p. 188.
- ¹⁸T. Jiang, Q. Cui, G. Shi, and S. Ma, *J. Chem. Phys.* **119**, 4592 (2003).
- ¹⁹F. Seno, M. Vendruscolo, A. Maritan, and J. R. Banavar, *Phys. Rev. Lett.* **77**, 1901 (1996).
- ²⁰R. Ramakrishnan, B. Ramachandran, and J. F. Pekny, *J. Chem. Phys.* **106**, 2418 (1997).
- ²¹A. Irbäck, C. Peterson, F. Potthast, and E. Sandelin, *Phys. Rev. E* **58**, R5249 (1998).
- ²²L. W. Lee and J.-S. Wang, *Phys. Rev. E* **64**, 056112 (2001).
- ²³G. Chikenji, M. Kikuchi, and Y. Iba, *Phys. Rev. Lett.* **83**, 1886 (1999), and references therein.
- ²⁴M. N. Rosenbluth and A. W. Rosenbluth, *J. Chem. Phys.* **23**, 356 (1955).
- ²⁵D. Aldous and U. Vazirani, in *Proceedings of the 35th Annual Symposium on Foundations of Computer Science*, Santa Fe (IEEE, Los Alamitos, 1994), p. 492.
- ²⁶P. Grassberger and W. Nadler, in *Computational Statistical Physics-From Billiards to Monte Carlo*, edited by K. H. Hoffmann and M. Schreiber (Springer, Berlin, 2002), p. 169, and references therein.
- ²⁷P. Grassberger, *Phys. Rev. E* **56**, 3682 (1997); H. Frauenkron, U. Bastolla, E. Gerstner, P. Grassberger, and W. Nadler, *Phys. Rev. Lett.* **80**, 3149 (1998); U. Bastolla, H. Frauenkron, E. Gerstner, P. Grassberger, and W. Nadler, *Proteins* **32**, 52 (1998).
- ²⁸H.-P. Hsu, V. Mehra, W. Nadler, and P. Grassberger, *J. Chem. Phys.* **118**, 444 (2003); *Phys. Rev. E* **68**, 021113 (2003).
- ²⁹M. Bachmann and W. Janke, *Phys. Rev. Lett.* **91**, 208105 (2003).
- ³⁰M. Bachmann and W. Janke, *J. Chem. Phys.* **120**, 6779 (2004).
- ³¹R. J. Najmanovich, J. L. deLira, and V. B. Henriques, *Physica A* **249**, 374 (1998).
- ³²E. E. Lattman, K. M. Fiebig, and K. A. Dill, *Biochemistry* **33**, 6158 (1994).
- ³³L. Toma and S. Toma, *Protein Sci.* **5**, 147 (1996).
- ³⁴S. Miyazawa and R. L. Jernigan, *J. Mol. Biol.* **256**, 623 (1996).
- ³⁵In contrast to Ref. 2, we have kept $u_{HH}^{MHP} = u_{HH}^{HP} = -1$ and rescaled the value of u_{HP}^{MHP} by the factor of 2.3. This number was chosen in Ref. 2 as a result of an analysis for the interresidue energies of contacts between hydrophobic amino acids and contacts between hydrophobic and polar residues (Ref. 34) which motivated the relation $2u_{HP} > u_{PP} + u_{HH}$.
- ³⁶D. S. Gaunt and A. J. Guttmann, *Asymptotic Analysis of Coefficients*, in *Phase Transitions and Critical Phenomena*, Vol. 3, edited by C. Domb and M. S. Green (Academic, London, 1974), p. 181.
- ³⁷J. L. Guttmann and A. J. Guttmann, *J. Phys. A* **26**, 2485 (1993).
- ³⁸See, e.g., H. E. Stanley, *Introduction to Phase Transitions and Critical Phenomena* (Oxford University Press, New York, 1987); A. J. Guttmann, *Asymptotic Analysis of Power-Series Expansions*, in *Phase Transitions and Critical Phenomena*, Vol. 13, edited by C. Domb and J. L. Lebowitz (Academic, London, 1989), p. 3.
- ³⁹D. MacDonald, D. L. Hunter, K. Kelly, and N. Jan, *J. Phys. A* **25**, 1429 (1992).
- ⁴⁰D. MacDonald, S. Joseph, D. L. Hunter, L. L. Moseley, N. Jan, and A. J. Guttmann, *J. Phys. A* **33**, 5973 (2000).
- ⁴¹M. Chen and K. Y. Lin, *J. Phys. A* **35**, 1501 (2002).
- ⁴²S. Caracciolo, A. S. Causo, and A. Pelissetto, *Phys. Rev. E* **57**, R1215 (1998).
- ⁴³R. Guida and J. Zinn-Justin, *J. Phys. A* **31**, 8103 (1998).
- ⁴⁴M. Vendruscolo and E. Domany, *Folding Des.* **2**, 295 (1997); **3**, 329 (1998).
- ⁴⁵R. Schiemann, M. Bachmann, and W. Janke, *Comput. Phys. Commun.* **166**, 8 (2005).
- ⁴⁶E. G. Emberly, J. Miller, C. Zeng, N. S. Wingreen, and C. Tang, *Proteins* **47**, 295 (2002).
- ⁴⁷H. Li, R. Helling, C. Tang, and N. Wingreen, *Science* **273**, 666 (1996).
- ⁴⁸L. H. Wong and A. L. Owczarek, *J. Phys. A* **36**, 9635 (2003).
- ⁴⁹M. Bachmann and W. Janke, *Acta Phys. Pol. B* **34**, 4689 (2003).